Amalgamation of copper nanoparticles of assorted size using *Nelumbo nucifera* (lotus) leaf and its bioelectrical assay

R Jeeffin Blessikha* & C Isac Sobana Raj

Department of Chemistry & Research, Nesamony Memorial Christian College, Marthandam 629 165,
Tamil Nadu, India.
Affiliated to Manonmaniam Sundaranar University, Abishekapatti, Tirunelveli 627 012, Tamil Nadu, India.

E-mail: blessikhajeeffin@gmail.com

There are several potential uses for green nanoparticle amalgamated in the medicinal and environmental sciences. Green synthesis specifically tries to reduce the use of harmful chemicals. For instance, it is often acceptable to employ organic resources like plants. In a single green synthesis step, biomolecules found in plant extract may transform metal ions into nanoparticles. This naturally occurring conversion of a metal ion to a base metal may be carried out quickly, conveniently, and at ambient temperature and pressure. In the current study, the production of CuNPs utilizing different-sized *Nelumbo nucifera* leaf extract has been reported. In order to determine how CuNPs generated, several techniques including UV-Visible, XRD, SEM, EDAX, FTIR, and cyclic voltammetry studies were used. The UV-Visible spectra of the amalgamated CuNPs show a peak between 250 and 450 nm. The morphology of CuNPs are spike in shapes with sizes of 33nm for 10mM and 25nm for 50mM, and the nanoparticles are crystalline in nature, according to the XRD and SEM examinations. The amalgamated CuNPs contain 37.55% copper, according to EDAX, and FTIR shows the absorption peak of copper at 1640 and 576 cm^{-1}.The oxidation and reduction of amalgamated CuNPs are visible by cyclic voltammetry. CuNPs have been put to the test against *Staphylococcus aureus, Staphylococcus epidermidis, Klebsiella pneumoniae, Escherichia coli,* and *Pseudomonas aeruginosa* for their antibacterial properties. CuNPs show the greatest zone of inhibition when used against *Pseudomonas aeruginosa*. *Aspergillus flavus* and *Candida albicans* have been used as test subjects for the antifungal testing of CuNPs. The CuNPs against *Candida albicans* show the largest zone of inhibition. CuNPs demonstrate strong antibacterial and antifungal efficacy, which means they have a considerable potential for application in the development of medications used to treat bacterial and fungal infections. The electrical potential difference of amalgamated CuNPs has been measured using a voltmeter and it is found that as concentration rises, so does the electrical potential difference.

Keywords: Copper nanoparticles, *Nelumbo nucifera,* Cyclic Voltammetry, Antibacterial assay, Antifungal assay, Electrical potential difference

Nanotechnology holds an extensive application in the areas including medical science, textiles, material science, environmental conservation, chemical units, electronics and opto electronic devices[1-6]. Particularly, green synthesis is an environmental friendly and economical approach for the preparation of nanoparticles. Since, they does not comprise the employment or generation of toxic chemicals[7]. Among various metal oxide nanoparticles like Ni, Zn, Av and Fe, Copper nanoparticles was regarded as an optimistic material and it can be effectively employed in sections such as biomedical, industrial, electronics and antimicrobial products[8]. Green synthesis of CuNPs using plant extract have been generally applied in biomedical sciences for the treatment of many diseases. Moreover, plant mediated synthesis of CuNPs have receives wide attention because of its low toxicity and low time of consumption. During the preparation of CuNPs, plants behave as a good reducing and capping agent in the reduction of Cu ions intoCuNPs[9]. The majority of them combined copper nanoparticles in the green method[10-18].

In order to amalgamate copper nanoparticles in 2022, Jayarambab Naradala, Akshaykranth Allam, Venkatappa Rao Tumu, and Rakesh Kumar Rajaboina introduced 25mL of Bambusa arundinacea leaves extract to the cupric acetate solution and stirred it at 65°C for 4 hours[19]. The goal of the current effort is to combine copper nanoparticles of various sizes, without heating the solution.

In the present study, we have exhibited the synthesis of CuNPs using *Nelumbo nucifera* leaf extract. No one has amalgamated CuNPs using *Nelumbo nucifera* leaf extract. This *Nelumbo nucifera* is an aquatic plant with medicinal values and was found in India and China. It was reported that, it posses anti-diarrheal and antimicrobial properties[20]. The prepared copper nanoparticles were characterized by UV, XRD, SEM, EDAX, FTIR and Cyclic Voltammetry. Moreover, the antibacterial activity of the synthesized CuNPs has also been discussed against *Staphylococcus aureus, Staphylococcus epidermidis, Klebsiella pneumoniae, Escherichia coli,* and *Pseudomonas aeruginosa* and antifungal activity against *Aspergillus flavus* and *Candida albicans.* Finally electric potential difference was also done.

Experimental Section

Materials

Nelumbo nucifera leaves were purchased from shop. Analytic grade Copper (II) sulphate pentahydrate ($CuSO_4.5H_2O$) was purchased from Metis Industries, Navkar Chemical Compound C-1, 41/2, GIDC Estate, Kalol (N.G) 382725, Gandhinagar, while, Sodium hydroxide (NaOH) was purchased from Pabitra Exports, Ahmedabad, Gujarat, India.

Preparation of *Nelumbo nucifera* leaf juice

The leaves of *Nelumbo nucifera* we*re washed well and cut into small pieces. At 80°C, 5 g of powdered leaves were boiled with 100 mL of double distilled water for 30 min. The juice was then filtered using Whatman No. 1 filter paper before being analysed.

Amalgamation of Copper nanoparticles

A 100 mL solution of Copper (II) sulphate pentahydrate was made at a specified concentration (10, 20, 30, 40, and 50 mM)[21-24]. Add 100 mL of 10 mM sodium hydroxide solution to this solutions. Finally, 10 mL of juice from *Nelumbo nucifera* leaves was added to each beaker. At room temperature, the solution was stirred magnetically for 3 h. The solution was centrifuged at 2000 rpm for 15 min after it had been incubated for 24 h. To eliminate contaminants, the copper nanoparticles were rinsed twice with distilled water before being cleaned with ethanol. The copper nanoparticles are dried in an 80°C hot air furnace before being employed in further testing.

Characterization of amalgamated Copper nanoparticles

The characterization of amalgamated green copper nanoparticles was done by techniques such as Ultraviolet – Visible spectroscopy, Scanning electron microscope, Energy dispersive X-ray, X-ray diffraction and Fourier transformation infrared spectroscopy. UV-Vis spectroscopy is used for the detection of Surface Plasmon Resonance (SPR), which is a result of the electron band of the surface of metal nanoparticles resonating with light wave, X-ray diffraction (XRD) is used to identify the crystallographic shape of nanoparticles and crystalline particle size, Scanning Electron Microscope (SEM) was used to identify size, aggregation, and morphological forms of nanoparticles, Energy-dispersive spectroscopy (EDAX) was used to examine the purity and elemental makeup of green synthetic nanoparticles, Fourier transformation infrared spectroscopy (FTIR) was used identify the functional groups that reduce, cap, and the stabilize metal nanoparticles[25] and Cyclic Voltammetry (CV) was used to find oxidation and reduction of the reaction.

Biological activity of copper nanoparticles

The possible anti-bacterial activity of the amalgamated CuNPs was appraised against *Staphylococcus aureus, Klebsiella pneumonia, Escherichia coli, Pseudomonas aeruginosa* and *Staphylococcus epidermidis*. And the anti-fungal activity was appraised against *Aspergillus flavus* and *Candida albicans*. Mueller Hinton Agar (g/L) (Beef, infusion form – 300, casein acid hydrolysate– 17.5, starch – 1.5 and agar – 17) was prepared in Erlenmeyer flask. The material, as well as the pipette, Petri dishes and metallic borer was sterilized for 15 min at 121°C in an autoclave. Finally, under sterile conditions, the culture mixture was put into Petri dishes. To reach a final concentration of 20 mg/mL, all solvent extracts were diluted in 100 percent dimethyl sulfoxide (DMSO). The activity of a 20 μL sample was measured. Amikacin (10 μg) was used as the positive control and dimethyl sulfoxide (DMSO) was used as the negative control. At 37°C, all plates were incubated for 24 h.

Electrical potential

The electrical potential difference between two locations in an electric circuit is measured using a voltmeter. The voltmeter is connected in parallel to the electrical circuit in order to measure the potential difference. Both direct and alternating electric current are measured using it. A voltmeter is a current-controlled device, which implies that in order for it to work, there must be current. The unit of voltmeter is millivolt, kilovolt, and volt.

Results and Discussion

Visual Representation

The formation of CuNPs were confirmed by change of colour from blue to brown. Brown colour is produced as a result of the reduction of Cu^+ ions (Fig. 1).

UV Visible Spectroscopy

The UV spectroscopy of *Nelumbo nucifera* leaf juice shows absorption peak at 364 nm. The spectra of amalgamated CuNPs in different size shows absorption peak between 250 and 450 nm is due to the surface plasmon band of Cu revealed in Fig. 2.

X-ray diffraction

X-ray diffraction pattern of amalgamated CuNPs were carried out using a Bruker D8 advance X-ray diffractometer (XRD) with Cu-Kα radiation 40mA with a scanning rate of 2 min^{-1} of 10mM and 50mM solution is shown in Figs 3(a) and (b). The average particle size of amalgamated CuNPs is determined using Debye Scherrer equation. The size of CuNPs for concentration 10mM is 33nm and for 50mM is 25nm.

The sharp peak in both spectrum shows that the amalgamated CuNPs is crystalline in nature. The percentage of crystallinity of CuNPs for concentration 10mM is 92% and for 50mM is 87%. The BET surface area for concentration 10mM is 19.9 m^2/g and for 50mM is 26.36 m^2/g. The result show that when the concentration increases the size of the CuNPs decreases.

Scanning Electron Microscope

The morphology of amalgamated CuNPs of concentration 10mM is determined by SEM using model Joel's 5800 LV. The sample of concentration 10mM were placed in an evacuated chamber and scanned with an electron beam in a regulated pattern. The SEM image shows that the amalgamated CuNPs were spike in morphology. The magnification power of 3300, 7000 and 10,000 is shown in Fig. 4. The average particle size of CuNPs of concentration 10mM was confirmed by histogram of SEM image.
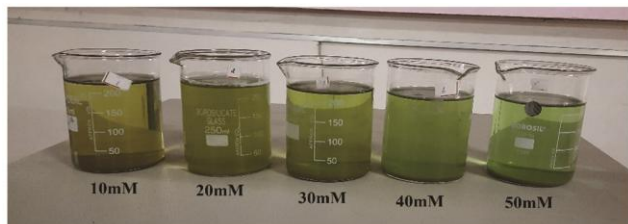

Fig. 1 — Visual representation of amalgamated copper nanoparticles
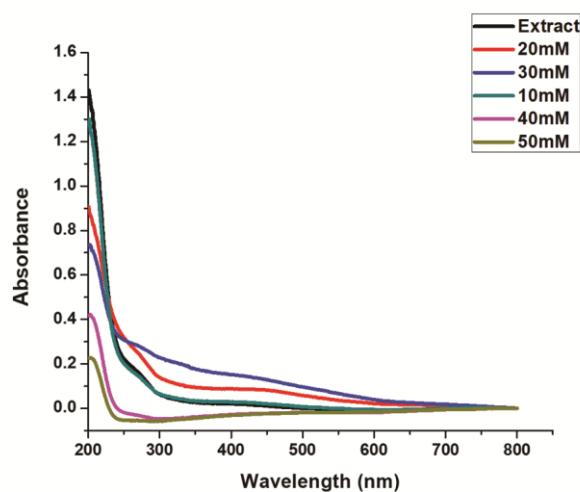

Fig. 2 — UV of *Lawsonia inermis* leaves juice, Copper nanoparticles synthesized from different concentration of copper (II) sulphate pentahydrate (10, 20, 30, 40 and 50mM)
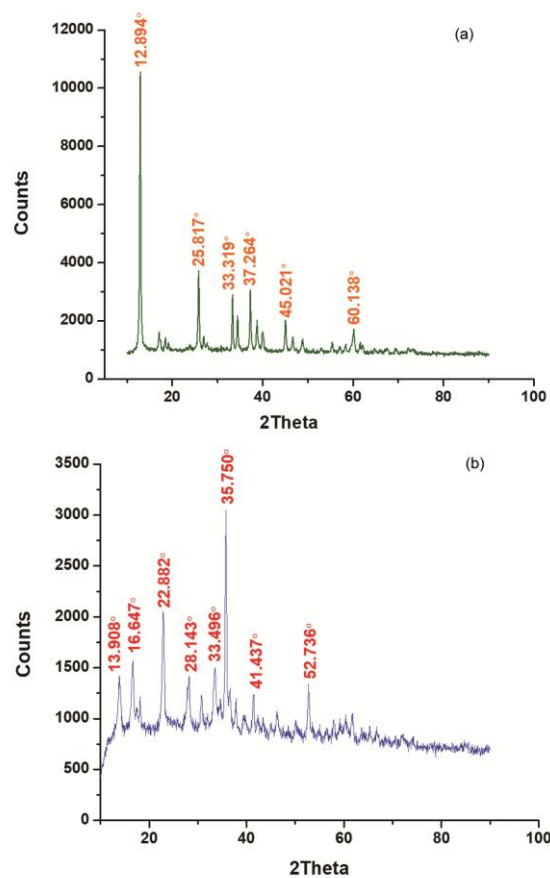

Fig. 3 — XRD spectrum of copper nanoparticles synthesized from (a) 10mM of Copper (II) sulphate pentahydrate and (b) 50mM of Copper (II) sulphate pentahydrate
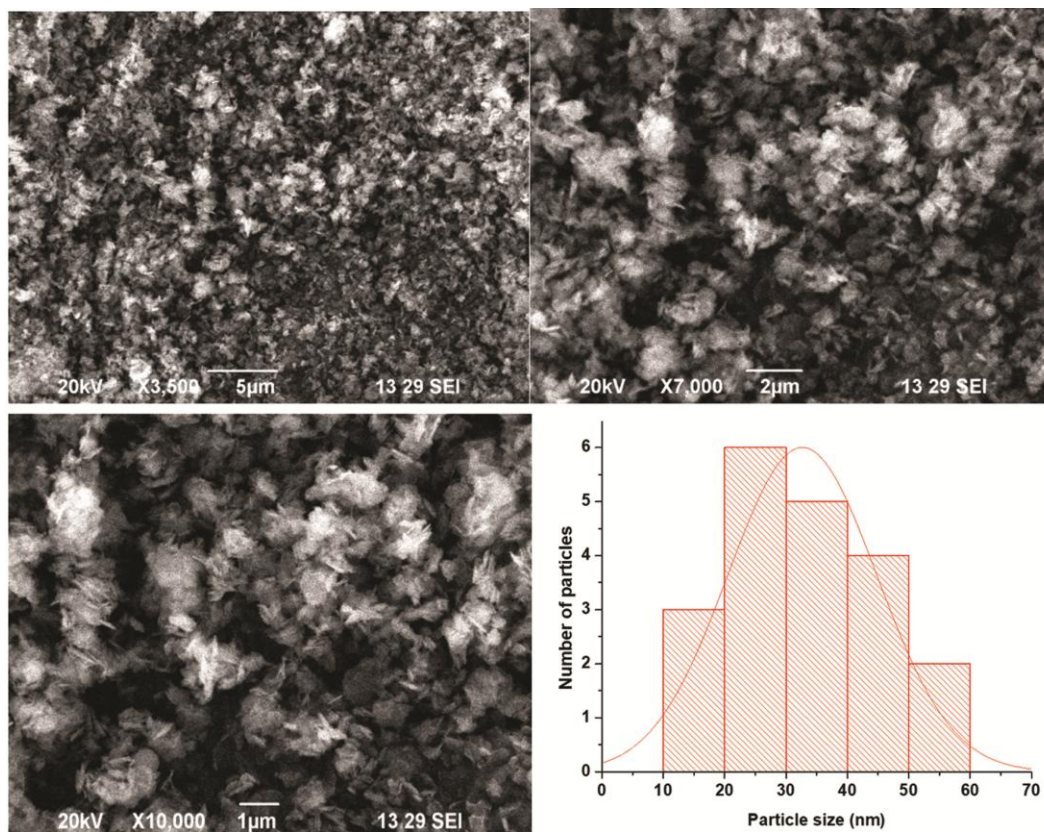
Fig. 4 — SEM image of copper nanoparticles synthesized from 10Mm of Copper (II) sulphate pentahydrate

Energy-dispersive spectroscopy

The composition of CuNPs was determined by energy-dispersive X-ray analysis of model JSM – 7100F. Figure 5 shows the EDAX spectrum of CuNPs obtained from 10Mm of solution. The spectrum indicate the pure copper (37.55%) was present in CuNPs.

Fourier transformation infrared spectroscopy

To identify the molecules responsible for reducing and for the formation of CuNPs FT-IR spectroscopy is used. The analysis was examined for concentration 10Mm of CuNPs amalgamated using Nelumbo nucifera leaf juice extract (Fig. 6 and Table 1). The peak absorbed at 1640 cm^{-1} and 576 cm^{-1} shows the presence of Cu[26-40].

Cyclic Voltammetry

Using a traditional three-electrode setup, CH Instruments Model 600E series carried out a Cyclic Voltammetry (CV) investigation. Glassy carbon electrode was used as the working electrode, Ag/AgCl electrode as the reference electrode, and platinum electrode as the counter electrode. Figure 7 illustrate a cyclic voltammetry curve for amalgamated CuNPs at

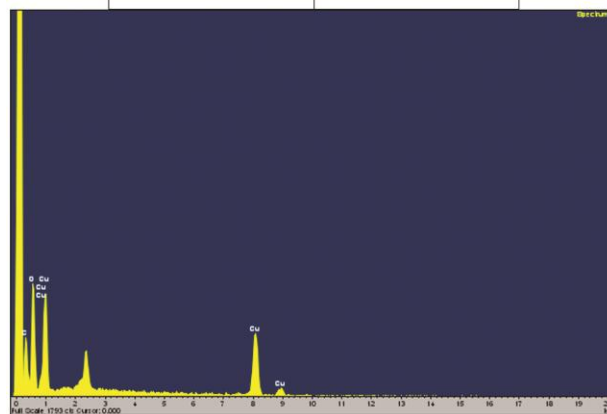| Element	Weight%
C	24.21
O	38.24
Cu	37.55

Fig. 5 — EDAX image of copper nanoparticles synthesized from 10Mm of Copper (II) sulphate pentahydrate

various concentrations (10, 20, 30, 40, and 50mM). The curve exhibits a clearly defined cathodic peak when the scan is directed towards negative potentials,
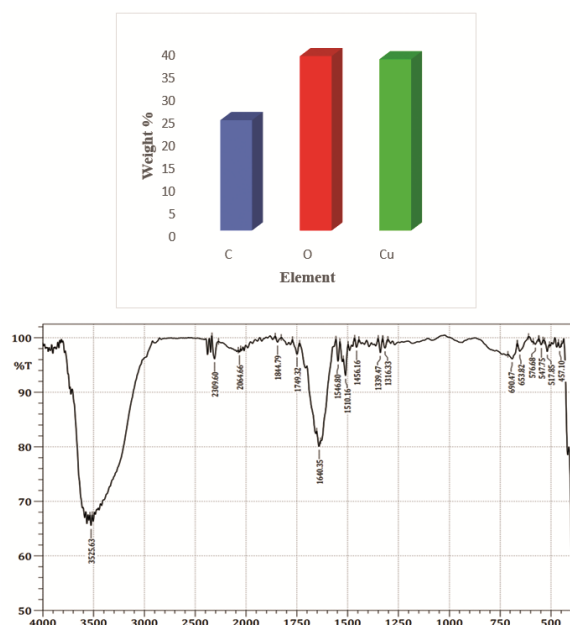
Fig. 6 — FT-IR spectrum of copper nanoparticles synthesized from 10mM of Copper (II) sulphate pentahydrate

Table 1 — FT-IR spectral data of copper nanoparticles synthesized from 10mM of Copper (II) sulphate pentahydrate

Sl. no	Absorption peak (cm^{-1})	Functional groups
1	3525	N-H streaching of amide
2	2309	Atmospheric CO_2
3	2064	Cu-H (Metal hydrogen) bonds
4	1844	Intensification of the carbonyl streaching vibration
5	1749	Carbonyl C=O streaching vibration
6	1640	Cu
7	1546	Streaching C=C
8	1510	C-N streaching of the aromatic amino group
9	1456	C-O-O streaching bands
10	1339	C-H bending vibrations due to alkanes
11	1316	C-O of ester
12	690	CH_3OH
13	653	Halogen compound
14	576	Cu
15	547	NC=N
16	517	C-N streaching vibration of straight chain alkyl halides
17	457	Cu-O streaching

and it clearly defined anodic peak when the scan is reversed. The reduction of Cu^{2+} to Cu and Cu to Cu^{2+} is responsible for the cathodic and anodic peaks,
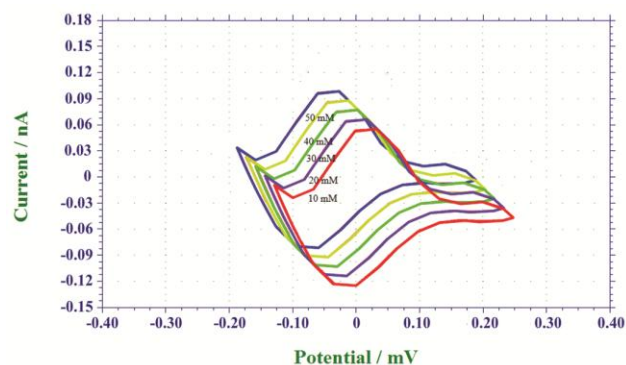

Fig. 7 — Cyclic Voltammetry of CuNPs at various concentrations

Table 2 — The variation of zone of inhibitions for different bacterial pathogens by Copper nanoparticles

Bacteria Name	Zone of inhibition (mm)					
	Concentration level					
	10mM	20mM	30mM	40mM	50mM	Standard
Staphylococcus aureus	7	7	11	12	12	30
Klebsiella pneumonia	7	9	10	14	14	16
Escherichia coli	7	9	9	10	12	30
Pseudomonas aeruginosa	7	12	10	13	15	30
Staphylococcus epidermidis	7	9	12	12	14	16

respectively. It also demonstrates that the current rises along with concentration.

Antibacterial assay

The antibacterial activity in this study was valuated by disc diffusion method against bacteria like *Staphylococcus aureus, Klebsiella pneumonia, Escherichia coli, Pseudomonas aeruginosa* and *Staphylococcus epidermidis.* The antibacterial activity of amalgamated CuNPs at various concentration (10, 20, 30, 40, and 50mM) is shown in Table 2 shows the variation in zone of inhibition. It was established that *Pseudomonas aeruginosa* was the most active bacteria followed by *Klebsiella pneumonia* [41,42], *Staphylococcus epidermidis, Escherichia coli* and *Staphylococcus aureus.* When the concentration increases the zone of inhibition also increases and it has a chance to reach the standard value[43].

Antifungal assay

The antifungal activity in this study was valuated by disc diffusion method against fungi like *Aspergillus flavus* and *Candida albicans.* The antifungal activity of amalgamated CuNPs at various concentration 10, 20, 30, 40, and 50mM) is shown in

Table 3 — The variation of zone of inhibitions for different fungal pathogens by Copper nanoparticles

Fungi Name	Zone of inhibition (mm)					
	Concentration level					
	10mM	20mM	30mM	40mM	50mM	Standard
Aspergillus flavus	7	7	7	7	9	20
Candida albicans	7	9	12	25	29	32

Table 4 — The reading of electrical potential difference of synthesized copper nanoparticles by voltmeter

Concentration (mM)	Electrical potential difference (volt)
10	2.8
20	3.9
30	4.2
40	5.1
50	5.4

Table 3 shows the variation in zone of inhibition. It was established that *Candida albicans*[44] was the most active fungi than *Aspergillus flavus.* When the concentration increases the zone of inhibition also increases and it has a chance to reach the standard value.

Electrical potential

A voltmeter is used to measure the difference between amalgamated copper nanoparticles. In a rectangular dish about 10mL of copper nanoparticles is poured. By connecting a voltmeter, a battery, and a rectangular dish, the electrical potential difference is assessed. Finally, the outcome demonstrates that when concentration rises, electrical potential difference rises as well (Table 4).

Conclusion

CuNPs were successfully amalgamated using a leaf extract from the medicinal plant *Nelumbo nucifera.* CuNPs have an absorption peak in the UV-Visible range between 250 and 450 nm. According to the morphology research, the CuNPs are shaped as spike, measuring 33 nm for 10 mM and 25 nm for 50 mM. Amalgamated CuNPs with a 37.55% Cu content were examined using EDAX spectra. FTIR was used to investigate the molecules reducing and producing CuNPs, and the results reveal that Cu has absorption peaks at 1640 and 576 cm^{-1}. The oxidation and reduction of CuNPs production are observable using cyclic voltammetry. The antibacterial and antifungal biosynthesized CuNPs exhibit maximal zones of inhibition in *Pseudomonas aeruginosa* bacteria and *Candida albicans* fungus, respectively. The electrical potential difference demonstrates that as concentration rises, similarly the electrical potential difference rises. This is because higher concentrations also have larger concentrations of copper. Due of copper's high electrical conductivity, there is a greater electrical potential difference. In view of all this, it can be said that the green synthesis has the potential to be highly important and successful for the creation of non-toxic, affordable, and environmentally friendly CuNPs.

Reference

1   Sreeja C K, Annieta Philip K, Shamil O P & Asraj S S, *J Nanosci Technol*, 6 (2020) 908.
2   Priyadharshini S S, Shubha J P, Shivalingappa J, Adil S F, Kuniyil M, Hatshan M R, Shaik B & Kavalli K, *Crystals*, 12 (2022) 22.
3   Sukumar S, Rudrasenan A & Nambiar D P, *ACS Omega*, 5 (2020) 1040.
4   Mali S C, Dhaka A, Githala C K & Trivedi R, *Biotechnol Rep*, 27 (2020) 1.
5   Jayandran M, Haneefa M M & Balasubramanian V, *J Appl Pharm Sci*, 5 (2015) 105.
6   Mohammed A A, Hassan A K & Kadhim F Q, *Iraq J Sci*, 62 (2021) 2833.
7   Amjad R, Mubeen B, Ali S S, Imam S S, Alshehri S, Ghoneim M M, Alzarea S L, Rasool R, Ullah I, Nadeem M S & Kazmi I, *Polymers*, 13 (2021) 4364.
8   Liu H, Wang G, Liu J, Nan K, Zhang J, Guo L & Liu Y, *J Exp Nanosci*, 16 (2021) 410.
9   Abdallah B M & Ali E M, *Am Chem Soc*, 6 (2021) 8151.
10 Amjad R, Mubeen B, Ali S S, Imam S S, Alshehri S, Ghoneim M M, Alzarea S I, Rasool R, Ullah I, Ghoneim M S N & Kazmi I, *Polymers*, 13 (2021) 4364.
11 Al Banna L S, Salem N M, Jaleel G A & Awwad A M, *Chem Int*, 6 (2020) 137.
12 Chandraker S K, Lal M, Ghosh M K, Tiwari V, Ghorai T K & Shukla R, *Nano Express*, 1 (2020) 10.
13 Izionworu V O, Ukpaka C P & Oguzie E E, *Chem Int*, 6 (2020) 232.
14 Tshireletso P, Ateba C N & Fayemi O E, *Molecules*, 26 (2021) 586.

15 Ali K, Saquib Q, Ahmed B, Siddiqui M A, Ahmad J, Al-Shaeri M, Al-khedhairy A A & Musarrat J, *Process Biochem*, 91 (2020) 387.

16 Sukumar K, Arumugan S, Thangaswamy S, Balakrishnan S, Chinnappan S & Kandasamy S, *Optik*, 202 (2020) 163507.

17 Velsankar K, Kumar R M A, Preaching R, Muthulakshmi V & Sudhahar S, *J Environ Chemi Eng*, 8 (2020) 8.

18 Zhao H, Su H, Ahmeda A, Sun Y, Li Z, Zangeneh M M, Nowrozi M, Zangeneh A & Moradi R, *Appl Organ Chem*, 36 *(*2020) e5587.

19 Naradala J, Allam A, Tumu V R & Rajaboina R K, *Biointerf Res Appl Chem*, 12 (2022) 1230.

20 Premanand G, Shanmugam N, Kannadasan N, Sathishkumar K & Viruthagiri G, *Appl Nanosci*, 6 (2016) 409.

21 Aher H R, Han S H, Vikhe A S & Kuchekar S R, *Chem Sci Trans*, 8 (2019) 1.

22 Lee H J, Lee G, Jang N R, Yun J H, Song J Y & Kim B S, *NSTI-Nanotech*, 1 (2011) 371.

23 Jahan I, Erci F & Isildak I, *J Drug Deliv Sci Technol*, 61 (2020) 102172.

24 Bale V K & Katreddi H R, *Int J Nano Dimens*, 13 (2022) 1214.

25 Salem S S & Fouda A, *Biolog Trace Element Res*, 199 (2020) 344.

26 Kushwaha S & Prakash P, *Int J Res Appl Sci Eng Technol*, 9 (2021) 1205.

27 Ananda M H C, Desalegn T, Kassa M, Abebe B & Assefa T, *J Nanomater*, 2020 (2020) 1.

28 Kausar H, Mehmood A, Khan R T, Ahmad K S, Hussain S & Nawaz F, Iqbal M S, Nasir M & Ullah T S, Green synthesis and characterization of copper nanoparticles for investigating their effect on germination and growth of wheat., *PLoS ONE*, 17 (2022) 1.

29 Wenig R W & Schrader G L, *J Phys Chem*, 91 (1987) 91911.

30 Abderrahim B, Abderrahman E, Mohamed A, Faima T, Abdesselam T & Krim O, *World Journal Environ Eng*, 3 (2015) 95.

31 Betancourt-Galindo R, Reyes-Rodriguez P Y, Puente-Urbina B A, Avila-Orta C A, Rodriguez-Fernandez O S, Cadenas-Pliego G, Lira-Saldivar R H & Garcia-Cerda L A, *J Nanomater*, 2014 (2014) 1.

32 Seyedeh Maryam H & Dehghannya J, *Part Sci Technol*, 38 (2020) 1019.

33 Saif S, Tahr A, Asim T & Chen Y, *Nanomaterials*, 6 (2016) 205.

34 Jabli M, Al Ghamdi Y O, Sebeia N, Almalki S G, Alturaiki W, Khaled J M, Mubarak A S & Algethami F K, *Mater Chem Physics*, 249 (2020) 1.

35 White D W, Gerakines P A, Cook A M & Whittet D C B, *Astrophys J Suppl Ser*, 180 (2019) 182.

36 Vijayakumar S, Arulmozhi P, Kumar N, Sakthivel B, Prathip K S & Praseetha P K, *Mater Today: Proceed*, 23 (2019) 73.

37 Thiruvengadam M, Chung I M. Gomathi T, Ansari M A, Khanna V G, Babu V & Rajakumar G, *Bioprocess Biosyst Eng*, 42 (2019) 41769.

38 Ramos J M, de M Cruz M T, Costa Jr A C, Versiane O & Tellez S C A, *Sci Asia*, 37 (2011) 247.

39 Tahir K, Nazir S, Li B, Khan A U, Khan Z U H, Gong P Y, Khan S U & Ahmad A, *Mater Lett*, 156 (2015) 198.

40 Keabadile O P, Aremu A O, Elugoke S E & Fayemi O E, *Nanomaterials*, 10 (2020) 2502.

41 Angrasan J & Subbaiya R, *Int J Curr Microbial Appl Sci*, 3 (2014) 768.

42 Gopinath M, Subbaiya R, Selvam M M & Suresh D, *Int J Curr Microbial Appl Sci*, 3 (2014) 814.

43 Ananthi P & Mary J K S, *Int J Innov Res Sci Eng Technol*, 6 (2017) 13455.

44 Jayandran M, Muhamed H M & Balasubramanian V, *J Chem Pharm Res*, 7 *(*2015) 251.